



Cite this: *Chem. Commun.*, 2023, 59, 4636

Received 15th February 2023,  
Accepted 14th March 2023

DOI: 10.1039/d3cc00572k

rsc.li/chemcomm

**The synthesis and characterization of a series of Mo(iv) bis- $\beta$ -diketonate ( $^R\text{diket}$ , R = Me,  $^t\text{Bu}$ , Ph) dichloride ( $^R\text{Mo}^{\text{IV}}\text{Cl}_2$ ) and bistriflate ( $^R\text{Mo}^{\text{IV}}(\text{OTf})_2$ ) complexes are reported. All complexes are characterized in solid and solution state by XRD and  $^1\text{H}$  NMR spectroscopy. We demonstrate that the bistriflate complexes constitute highly active catalysts for allylic substitution reactions.**

Understanding the chemical and reactivity properties of six-coordinate Mo(iv) complexes is key to a better understanding of a wide number of Mo-based enzymatic systems.<sup>1–4</sup> However, the vast majority of the reported six-coordinate Mo(iv) complexes are supported by neutral, strongly  $\pi$ -accepting donor ligands such as CO, NO or phosphines,<sup>5</sup> and only a handful of mononuclear six-coordinate Mo(iv) compounds bearing anionic oxygen or sulfur donating ligands have been reported in literature,<sup>6–10</sup> at the difference of much more common Mo(vi) counterparts. A case in point is the octahedral Mo(iv) bis-acetylacetone ( $^{\text{Me}}\text{diket}$ ) dichloride complex,  $[\text{Mo}^{\text{IV}}(^{\text{Me}}\text{diket})_2\text{Cl}_2]$  ( $^{\text{Me}}\text{Mo}^{\text{IV}}\text{Cl}_2$ ), early reported<sup>11–13</sup> but not structurally characterized. It was proposed to display *cis* coordination of the chloride ligands based on the analysis of IR stretches<sup>12,13</sup> and suggested to be a coordination polymer type structure<sup>11</sup> owing to its very low solubility.<sup>12,13</sup> Interestingly,  $^{\text{Me}}\text{Mo}^{\text{IV}}\text{Cl}_2$  was proposed to act as a pre-catalyst for allylic substitution reactions when combined *in situ* with silver salts, such as AgOTf (TfO = trifluoromethylsulfonate) or AgSbF<sub>6</sub>, (*vide infra*).<sup>14–17</sup> Nevertheless, the identity of the catalytically active species as well as the one generated upon addition of the silver salts had never been investigated. Here, we report the systematic preparation and characterization of a series of Mo(iv) complexes supported by  $\beta$ -diketonate ligands as well as the investigation of their catalytic activity for allylic substitution reactions. We found that while the parent Mo(iv) complexes are

Department of Chemistry and Applied Biosciences, Laboratory of Inorganic Chemistry, ETH Zurich, 8093 Zurich, Switzerland.

E-mail: mougel@inorg.chem.ethz.ch

† Electronic supplementary information (ESI) available. CCDC 2239585, 2240098–2240102. For ESI and crystallographic data in CIF or other electronic format see DOI: <https://doi.org/10.1039/d3cc00572k>

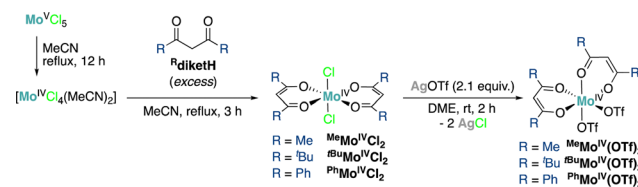
## Molybdenum(iv) $\beta$ -diketonate complexes as highly active catalysts for allylic substitution reactions†

Fabio Masero and Victor Mougel \*

the catalytically most active species, *in situ* generated higher valent Mo oxo and nitrido complexes also yield catalytically active species, yet performing at much lower rates. We show that the careful design of catalytic reaction conditions based on this mechanistic analysis enabled efficient and fast catalysis at low catalyst loading.

By analogy with the reported synthesis of  $^{\text{Me}}\text{Mo}^{\text{IV}}\text{Cl}_2$ ,<sup>12,13</sup> we explored here the preparation of a series of Mo(iv) dichloride bis- $\beta$ -diketonate ( $^R\text{diket}$ , R = Me,  $^t\text{Bu}$ , Ph, CF<sub>3</sub>) complexes by protonolysis of *in situ* generated  $[\text{MoCl}_4(\text{CH}_3\text{CN})_2]$  from  $[\text{MoCl}_5]$  in refluxing acetonitrile (MeCN), with the corresponding  $\beta$ -diketone ligand. The resulting  $^R\text{Mo}^{\text{IV}}\text{Cl}_2$  complexes were isolated in pure form in 49%, 47% and 67% yields for R = Me, Ph and  $^t\text{Bu}$  respectively (Scheme 1). Nevertheless, the complexes displayed significant differences in solubility: while for R = Me and Ph, highly insoluble materials were obtained, the use of  $^t\text{Bu}$  groups as terminal substituents on the diketonate ligand enabled significantly improving the solubility of the complex in common solvents such as toluene or tetrahydrofuran (THF), facilitating its purification, isolation and characterization. We did not succeed in isolating the targeted complex for R = CF<sub>3</sub> but instead identified products of a disproportionation reaction by single crystal X-ray diffraction (XRD, Fig. S3, ESI†). We hypothesize that the strong electron withdrawing properties of the CF<sub>3</sub>-substituted diketonate ligand do not allow stabilizing the electron-poor Mo(iv) complex.

Exchange of the chloride ligands with  $^-\text{OTf}$  anions was carried out *via* salt metathesis: addition of two equivalents of solid AgOTf to a solution (R =  $^t\text{Bu}$ ) or a suspension (R = Me, Ph)



Scheme 1 Synthesis of Mo(iv)  $\beta$ -diketonate complexes.



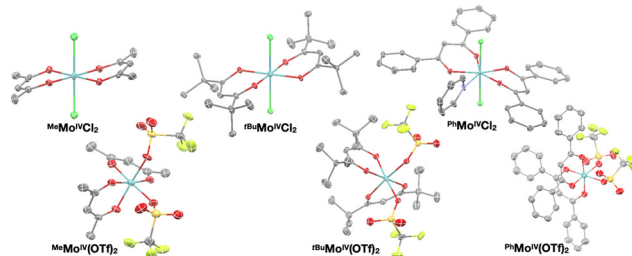


Fig. 1 Crystal structures of dichloride- (top) and bis triflate complexes (bottom). Ellipsoids are drawn at the 50% probability level and all hydrogen atoms were omitted for clarity.

of  ${}^{\text{R}}\text{Mo}^{\text{IV}}\text{Cl}_2$  in 1,2-dimethoxyethane resulted in the precipitation of  $\text{AgCl}$  as a colorless solid and the formation of red-orange solutions.<sup>‡</sup> Filtration followed by removal of volatiles under reduced pressure afforded the desired bis triflate ( ${}^{\text{R}}\text{Mo}^{\text{IV}}(\text{OTf})_2$ ) complexes ( $\text{R} = {}^{\text{t}}\text{Bu, Me, Ph}$ ) as bright red-orange solids in 71%, 86% and 76% yields, respectively. Reactions with  $\text{AgSbF}_6$ , previously used for the *in situ* generation of active catalysts for allylic substitution reactions,<sup>14</sup> yielded complex mixtures. We attempted to determine the identity of these reaction byproducts in the case of  $\text{R} = {}^{\text{t}}\text{Bu}$ , revealing the occurrence of ligand scrambling and oxidation of the complex (Fig. S4, ESI<sup>†</sup>).

The solid state structures of  ${}^{\text{R}}\text{Mo}^{\text{IV}}\text{Cl}_2$  ( $\text{R} = \text{Me, } {}^{\text{t}}\text{Bu, Ph}$ ) and  ${}^{\text{R}}\text{Mo}^{\text{IV}}(\text{OTf})_2$  ( $\text{R} = \text{Me, } {}^{\text{t}}\text{Bu, Ph}$ ) complexes were characterized by single crystal XRD (Fig. 1). All compounds were found to crystallize as mononuclear coordination complexes, enabling us to unambiguously disclose the initially proposed formulation of  ${}^{\text{Me}}\text{Mo}^{\text{IV}}\text{Cl}_2$  as a coordination polymer.<sup>11</sup> We observed that all the Mo(IV) dichloride complexes crystallized with the two chloride ligands *trans* to each other. Note that while both  ${}^{\text{Me}}\text{Mo}^{\text{IV}}\text{Cl}_2$  and  ${}^{\text{tBu}}\text{Mo}^{\text{IV}}\text{Cl}_2$  can be crystallized directly from the reaction mixture as distorted octahedral complexes with the two chloride ligands in apical positions with nearly identical bond metrics,  ${}^{\text{Ph}}\text{Mo}^{\text{IV}}\text{Cl}_2$  precipitates from the reaction mixture as a dark black amorphous powder. We only achieved growing suitable crystals for XRD analysis by slow diffusion of  ${}^{\text{n}}\text{pentane}$  into a saturated pyridine solution. The solid state structure yet revealed the presence of an additional equatorial pyridine ligand, giving rise to a seven-coordinate complex.

XRD analysis of the bis triflate complexes ( $\text{R} = \text{Me, } {}^{\text{t}}\text{Bu}$ ) showed that both complexes display distorted octahedral geometries where the two triflate ligands are positioned *cis* to each other, in contrast to the *trans* coordination geometry observed for their dichloride counterparts. Despite this change in coordination geometry, the  $\text{Mo}^{\text{IV}}-\text{O}(\text{Rdiket})$  average bond lengths are essentially identical when moving from the dichloride ( $d_{\text{Mo-O}} = 2.01 \text{ \AA}$ ) to the bis triflate ( $d_{\text{Mo-O}} = 1.97 \text{ \AA}$ ) complexes, and in the same range than in previously reported solid state structures of diketonate Mo complexes such as  $[\text{Mo}^{\text{III}}(\text{Me diket})_3]$ ,<sup>18,19</sup>  $[\text{Mo}^{\text{V}}\text{O}(\text{tBu diket})_2]_2-\mu\text{-O}$ <sup>20</sup> and  $[\text{Mo}^{\text{VI}}\text{O}_2(\text{Me diket})_2]$ <sup>21</sup> ( $\Delta d_{\text{Mo-O(diket)}} < 0.1 \text{ \AA}$ , see Table S6, ESI<sup>†</sup>). Worthy of note is the fact that, in the case of  ${}^{\text{Me}}\text{Mo}^{\text{IV}}\text{Cl}_2$ , the chelate formed by the diketonate ligand and the Mo center significantly deviates from planarity ( $\measuredangle = 21.4^\circ$ ), breaking up the complexes' overall  $D_{\text{4h}}$  symmetry

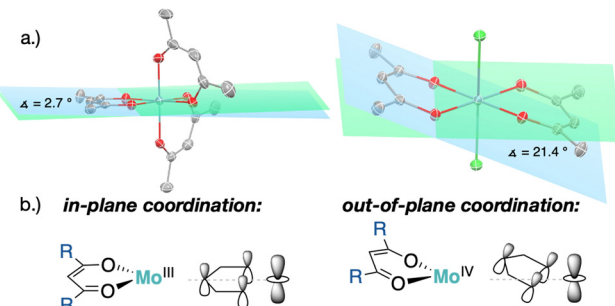


Fig. 2 (a) Solid state structures of  $[\text{Mo}^{\text{III}}(\text{Me diket})_3]$  (left)<sup>18</sup> and  ${}^{\text{Me}}\text{Mo}^{\text{IV}}\text{Cl}_2$  (right) with highlighted bending angle (ellipsoids at the 50% probability level, all hydrogens omitted for clarity), (b) qualitative molecular orbital interaction diagram for bent vs. linear  $\beta$ -diketonate coordination to Mo.

(Fig. 2a). We further identified that the chelate is nearly planar ( $\measuredangle = 4.2 \pm 1.1^\circ$ ) in lower-valent  $[\text{Mo}^{\text{III}}(\text{Me diket})_3]$ <sup>18,19</sup> while high-valent  $[\text{Mo}^{\text{VI}}\text{O}_2(\text{Me diket})_2]$ <sup>21</sup> displays a similar bending of the diketonate ligand ( $\measuredangle = 22.1^\circ$ ). We propose that this deviation results from a non-zero orbital overlap between the HOMO of the anionic  $\beta$ -diketonate ligand<sup>22</sup> and an empty orbital of appropriate symmetry of the metal fragment (an example with the  $d_{z^2}$  orbital is highlighted in Fig. 2b). Population of these empty orbitals upon reduction of the Mo center will disfavor this interaction, resulting in a more planar coordination mode of the  $\beta$ -diketonate ligand. The larger angle observed in the case of  ${}^{\text{tBu}}\text{Mo}^{\text{IV}}\text{Cl}_2$  ( $\measuredangle = 25.4^\circ$ ) is in line with the stronger electron-donating properties of the  ${}^{\text{t}}\text{Bu}$  groups of its supporting ligand, increasing its  $\pi$ -donation capabilities. DFT calculations further support this hypothesis, reproducing well the trend, yet at a smaller magnitude (see Sections S4 and S7, and Fig. S44, ESI<sup>†</sup>).

Both the Mo(IV) dichloride and bis triflate complexes are paramagnetic compounds, as highlighted by magnetic susceptibility measurements in both the solid and liquid state, suggesting a high spin  $d^2$  electronic configuration (Section S2, ESI<sup>†</sup>). Yet, this paramagnetic character did not impede the characterisation of the complexes by  ${}^1\text{H}$  and  ${}^{19}\text{F}$  (for bis-triflate complexes) NMR (Section S5, ESI<sup>†</sup>). In solution, both *cis*- and *trans*-isomers are observed for all the complexes synthesized, independently of the present  $\text{X}^-$  ligand ( $\text{X}^- = \text{Cl}^-$  or  $\text{TfO}^-$ ) (Fig. S20–S36, ESI<sup>†</sup>). As an exception, in MeCN, the most polar solvent studied here,  ${}^{\text{tBu}}\text{Mo}^{\text{IV}}(\text{OTf})_2$  was found to be uniquely present as its *cis* isomer.

Owing to its increased solubility, the following detailed solution studies were only performed for the  ${}^{\text{t}}\text{Bu}$ -substituted diketonate complexes but the close similitudes between the  ${}^1\text{H}$  and  ${}^{19}\text{F}$  NMR spectra of all three complex families let us infer that the same conclusions can be drawn for the whole series. The ratio between the *cis*- and *trans*-isomers determined by  ${}^1\text{H}$  NMR and summarized for  ${}^{\text{tBu}}\text{Mo}^{\text{IV}}\text{Cl}_2$  and  ${}^{\text{tBu}}\text{Mo}^{\text{IV}}(\text{OTf})_2$  in Table 1 appeared to be both dependent of the anionic  $\text{X}^-$  ligand and the solvent used. A significant influence of the polarity of the media on the *cis*:*trans* ratio was observed, with more polar solvents favoring the *cis* isomer. The behavior at different temperatures was studied using variable temperature NMR (Fig. S39–S41, ESI<sup>†</sup>). The  $\text{Cl}^-$  and  $\text{TfO}^-$  complexes displayed



Table 1 Stereoisomer (*cis* : *trans*) ratios at 298 K determined by  $^1\text{H}$  NMR

	C <sub>6</sub> D <sub>6</sub>	CD <sub>3</sub> Cl	CD <sub>2</sub> Cl <sub>2</sub>	CD <sub>3</sub> CN
<sup>t</sup> BuMo <sup>IV</sup> Cl <sub>2</sub>	1 : 2.1	1.2 : 1	2.7 : 1	4.9 : 1
<sup>t</sup> BuMo <sup>IV</sup> (OTf) <sub>2</sub>	1.2 : 1	2.5 : 1	10.7 : 1	<i>cis</i> only

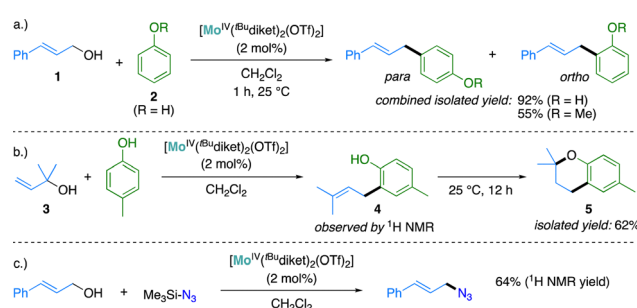
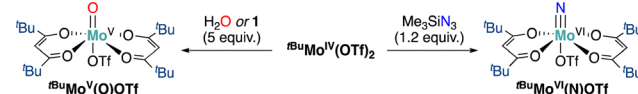
significantly different behavior: for <sup>t</sup>BuMo<sup>IV</sup>Cl<sub>2</sub> the *cis* : *trans* ratio is nearly independent on temperature, while for <sup>t</sup>BuMo<sup>IV</sup>(OTf)<sub>2</sub> the *cis* isomer is more favored at low temperature, in agreement with the *cis*-configuration observed in the single crystal structure. In case of the triflate complexes, structural information could be extracted from  $^{19}\text{F}$  NMR spectroscopy. Even in a coordinating solvent such as MeCN, the triflate ligands retain a characteristic  $^{19}\text{F}$  chemical shift (e.g.  $\delta \approx -40$  ppm for <sup>t</sup>BuMo<sup>IV</sup>(OTf)<sub>2</sub>), very distinct from free, non-coordinated  $^-\text{OTf}$  anions ( $\delta \approx -80$  ppm). This result suggests that the triflate ligands remain bound to Mo, in contrast to previous literature examples,<sup>23</sup> and highlights the strong Lewis acidity of the Mo center in this series.

We investigated the catalytic activity for allylic substitution reactions of the *in situ* generated mixtures in the presence of <sup>t</sup>BuMo<sup>IV</sup>Cl<sub>2</sub>/AgOTf (R = Me, Ph, <sup>t</sup>Bu) in a 1 : 2 ratio, using the coupling of cinnamyl alcohol (**1**) with electron-rich aromatics as carbon nucleophiles (e.g. phenol (**2**), anisole or *p*-cresol) as prototypical reactions. All three complexes proved efficient to promote the coupling (Section S3, ESI<sup>†</sup>). As no significant difference in catalytic activity could be detected with Mo(IV) complexes supported by the other  $\beta$ -diketonate ligands investigated here, we decided to restrict the more detailed reactivity and mechanistic studies to the most soluble complexes of the series, supported by <sup>t</sup>Bu-diket ligands.

Using <sup>t</sup>BuMo<sup>IV</sup>(OTf)<sub>2</sub> as a catalyst, full conversion was observed at a catalyst loading of 2 mol% within less than one hour at ambient temperature and the expected coupling products were isolated as mixtures of *ortho*- and *para* regio-isomers in good yields (92% for the coupling of **1** and **2**, Scheme 2a). The catalytic activity of <sup>t</sup>BuMo<sup>IV</sup>(OTf)<sub>2</sub> was further tested in a 3,3-cyclocoupling reaction of allylic alcohol **3** with *p*-cresol. This reaction – of interest to generate chroman moieties found notably in several pharmaceutical drugs<sup>24–26</sup> – may be described as a domino reaction, where an allylic substitution is followed by a Lewis acid-catalyzed cyclization step. This reaction was found challenging in the original report using the *in situ* generated catalyst

obtained with <sup>t</sup>BuMo<sup>IV</sup>Cl<sub>2</sub>/AgSbF<sub>6</sub> (1 : 2 ratio) mixtures, with a reported yield of only 27%.<sup>14</sup>  $^1\text{H}$  NMR analysis of the reaction using 2 mol% of <sup>t</sup>BuMo<sup>IV</sup>(OTf)<sub>2</sub> as a catalyst revealed the formation of the initial C–C coupling product **4** and its full conversion to the cyclized product **5** over prolonged reaction times (Scheme 2b and Fig. S5, S6, ESI<sup>†</sup>). Chroman **5** could be isolated in 62% yield, a significant improvement with respect to the previously reported yield obtained using *in situ* generated catalysts (*vide supra*). This reaction was previously reported to be catalyzed by Lewis<sup>27,28</sup> or Brønsted<sup>29</sup> acids under comparably harsher conditions, typically requiring elevated temperature (up to 150 °C), high catalyst loadings (5–15 mol%) or a large excess of *p*-cresol (up to 30 equiv.). To the best of our knowledge, the conditions for the preparation of chroman **5** described here (2 mol% catalyst loading, *p*-cresol (1.3 equiv.), 25 °C, no additives) are among the mildest reported to date.

Intrigued by the change of color of the reaction mixture from red to green under catalytic conditions, we attempted identifying the new species generated *in situ* and responsible of this color change. During the catalytic substitution of allylic alcohols, water (H<sub>2</sub>O) is expected as the main by-product. Here, we were able to show that [Mo<sup>V</sup>(O)(<sup>t</sup>Bu-diket)<sub>2</sub>(OTf)] (<sup>t</sup>BuMo<sup>V</sup>(O)OTf) is formed upon hydrolysis of <sup>t</sup>BuMo<sup>IV</sup>(OTf)<sub>2</sub> (Scheme 3). To probe this assumption, we independently investigated the reactivity of <sup>t</sup>BuMo<sup>IV</sup>(OTf)<sub>2</sub> with stoichiometric amounts of H<sub>2</sub>O. When a slight excess of H<sub>2</sub>O (5 equiv.) was added to a THF solution of <sup>t</sup>BuMo<sup>IV</sup>(OTf)<sub>2</sub>, a broad signal at 2.6 ppm appeared in the  $^1\text{H}$  NMR spectrum. Cooling this reaction mixture in acetonitrile at –35 °C afforded bright green crystals of <sup>t</sup>BuMo<sup>V</sup>(O)OTf (Fig. S19, ESI<sup>†</sup>). Interestingly, while the NMR and UV-Vis spectra of <sup>t</sup>BuMo<sup>IV</sup>(OTf)<sub>2</sub> do not change upon addition of (excess) **2**, addition of stoichiometric amounts of allylic alcohol **1** to <sup>t</sup>BuMo<sup>IV</sup>(OTf)<sub>2</sub> led to the fast appearance of the same broad signal at  $\delta = 2.6$  ppm in the  $^1\text{H}$  NMR spectrum of the mixture, pointing towards the *in situ* generation of <sup>t</sup>BuMo<sup>V</sup>(O)OTf (Fig. S18, ESI<sup>†</sup>). Relatedly,  $^1\text{H}$  NMR and UV-Vis spectra recorded *in situ* in the conditions used for the catalytic allylic substitution reaction of **1** with **2** (1 mol% <sup>t</sup>BuMo<sup>IV</sup>(OTf)<sub>2</sub>) confirm the fast formation of <sup>t</sup>BuMo<sup>V</sup>(O)OTf under catalytic conditions (Fig. S14 and S17, ESI<sup>†</sup>). Further, the conversion of the substrates is still observed when <sup>t</sup>BuMo<sup>V</sup>(O)OTf is the main Mo species, suggesting that it may also be catalytically active. To test this hypothesis, <sup>t</sup>BuMo<sup>V</sup>(O)OTf (1 mol%) was used as a catalyst for the allylic substitution of **1** with **2**. Full conversion was observed after 4 h at room temperature. However, *in situ*  $^1\text{H}$  NMR monitoring of the reaction revealed a much lower product formation rate, as if using <sup>t</sup>BuMo<sup>IV</sup>(OTf)<sub>2</sub> as the catalyst (Fig. S13, ESI<sup>†</sup>). A long induction period of *ca.* 40 min was observed, suggesting that <sup>t</sup>BuMo<sup>V</sup>(O)OTf is not the actual catalytically active species, but a resting state of

Scheme 2 Substitution of allylic alcohols with aromatic nucleophiles (a and b) and with trimethylsilyl azide (c) catalyzed by <sup>t</sup>BuMo<sup>IV</sup>(OTf)<sub>2</sub>.Scheme 3 Reactivity of <sup>t</sup>BuMo<sup>IV</sup>(OTf)<sub>2</sub> with allylic alcohol or H<sub>2</sub>O and TMSN<sub>3</sub>.

the catalyst. In addition, time-dependent UV-Vis spectroscopic studies carried out under catalytic conditions (Fig. S15, ESI<sup>†</sup>) did not exhibit significant changes over the course of the reaction, ruling out the *in situ* regeneration of the original Mo(iv) catalyst, and suggesting the formation of a new catalytically competent species. Assuming that the generation of the Mo(v) resting state is mainly driven by the accumulation of H<sub>2</sub>O released during the catalytic run, we attempted to optimize reaction conditions to prevent its formation. The presence of 4 Å molecular sieves (MS) as an additive to standard catalytic conditions using the Mo(iv) complex, led to much faster catalysis (98% conversion after 7 minutes, Fig. S12, ESI<sup>†</sup>). This suggests that the H<sub>2</sub>O by-product can be efficiently displaced by the MS, to significantly increase the lifetime of the Mo(iv) catalyst and disfavor the formation of Mo(v) oxo resting states. Based on these findings, we propose that under standard catalytic conditions, two separated catalytic cycles involving either the Mo(iv) or the Mo(v) complex as active species are operative (Scheme S2, ESI<sup>†</sup>), even though for catalyst loadings > 1 mol%, the latter can be neglected due to its comparably slow product formation rate.

<sup>tBu</sup>Mo<sup>IV</sup>(OTf)<sub>2</sub> is also an active catalyst promoting C–N bond formation reactions, enabling the formation of allylic azides (Scheme 2c and Fig. S7, ESI<sup>†</sup>). Interestingly, the catalytic reaction mixture did not display the characteristic change of color to green observed in C–C coupling reaction, but instead turned dark brown, suggesting the formation of at least one additional new species. We explored the reactivity of the second reactant, TMSN<sub>3</sub> (TMS = SiMe<sub>3</sub>) with <sup>tBu</sup>Mo<sup>IV</sup>(OTf)<sub>2</sub>. At the difference of 2, which did not display any significant reactivity with <sup>tBu</sup>Mo<sup>IV</sup>(OTf)<sub>2</sub>, a strong change of color to dark brown was observed immediately after addition of stoichiometric amounts of TMSN<sub>3</sub> (1.2 equiv.) to <sup>tBu</sup>Mo<sup>IV</sup>(OTf)<sub>2</sub>. Single crystal XRD measurements pointed to the formation of a new Mo(vi) species, namely [Mo<sup>VI</sup>(N)(<sup>tBu</sup>diket)<sub>2</sub>(OTf)](<sup>tBu</sup>Mo<sup>VI</sup>(N)OTf, Fig. S19, ESI<sup>†</sup>). The fact, that under catalytic conditions, TMSN<sub>3</sub> is present in large excess with respect to <sup>tBu</sup>Mo<sup>IV</sup>(OTf)<sub>2</sub>, suggests that the above-described reaction is likely to be present in significant amounts in catalytic conditions. Similarly to what observed with <sup>tBu</sup>Mo<sup>V</sup>(O)OTf, <sup>tBu</sup>Mo<sup>VI</sup>(N)OTf can catalyze allylic substitutions but is much more sluggish (*ca.* 25% conversion after 12 h, Fig. S8, ESI<sup>†</sup>) than the parent Mo(iv) complex.

The in-depth investigation of the coordination chemistry properties of a series of β-diketonate Mo(iv) complexes enabled to identify that the strongly Lewis acidic complexes <sup>R</sup>Mo<sup>IV</sup>(OTf)<sub>2</sub> are highly active catalysts for the substitution of allylic alcohols. Reactivity tests combined with *in situ* spectroscopic studies revealed that high-valent Mo(v) oxo or Mo(vi) nitrido complexes are quickly formed *in situ* under catalytic conditions. These species can also act as pre-catalysts for the targeted reactions, yet at the expense of much slower rates. This observation enabled to further rationally optimize reaction conditions to

lower the rate of formation of these species and respectively improve reaction rates and conversion.

We acknowledge funding from the European Research Council (ERC) under the European Union's Horizon 2020 research and innovation program (grant agreement no. 853064). We deeply thank Dr Michael Wörle, Dr René Verel, and Dr Christopher Gordon for their help with XRD, NMR, and DFT studies, respectively.

## Conflicts of interest

There are no conflicts to declare.

## Notes and references

<sup>‡</sup> When chloride triflate exchange reactions were performed in THF, rapid polymerization of the solution occurred, highlighting the high Lewis-acidity of the formed Mo(iv) triflate complexes.

1. R. Hille, J. Hall and P. Basu, *Chem. Rev.*, 2014, **114**, 3963–4038.
2. G. Schwarz, R. R. Mendel and M. W. Ribbe, *Nature*, 2009, **460**, 839–847.
3. L. B. Maia and J. J. Moura, *J. Biol. Inorg. Chem.*, 2015, **20**, 403–433.
4. L. B. Maia and J. J. Moura, *J. Biol. Inorg. Chem.*, 2011, **16**, 443–460.
5. C. G. Young, *Comprehensive Coordination Chemistry II*, Pergamon, 2003, pp. 415–527.
6. F. A. Cotton and G. Schmid, *Inorg. Chem.*, 1997, **36**, 2267–2278.
7. J. Bendix and A. Bogevig, *Inorg. Chem.*, 1998, **37**, 5992–6001.
8. E. Solari, C. Maltese, M. Latronico, C. Floriani, A. Chiesi-Villa and C. Rizzoli, *J. Chem. Soc., Dalton Trans.*, 1998, 2395–2400.
9. M. J. Bezdek and P. J. Chirik, *Dalton Trans.*, 2016, **45**, 15922–15930.
10. J. Song, Q. Liao, X. Hong, L. Jin and N. Mezaillies, *Angew. Chem., Int. Ed.*, 2021, **60**, 12242–12247.
11. M. L. Larson and F. W. Moore, *Inorg. Chem.*, 1964, **3**, 285–286.
12. G. Doyle, *Inorg. Chem.*, 1971, **10**, 2348–2350.
13. A. van den Bergen, K. S. Murray and B. O. West, *Aust. J. Chem.*, 1972, **25**, 705–713.
14. A. V. Malkov, P. Spoor, V. Vinader and P. Kocovsky, *J. Org. Chem.*, 1999, **64**, 5308–5311.
15. A. V. Malkov, B. P. Farn, N. Hussain and P. Kočovský, *Collect. Czech. Chem. Commun.*, 2001, **66**, 1735–1745.
16. A. V. Malkov and P. Kočovský, *Collect. Czech. Chem. Commun.*, 2001, **66**, 1257–1268.
17. B. Nay, M. Collet, M. Lebon, C. Chèze and J. Vercauteren, *Tetrahedron Lett.*, 2002, **43**, 2675–2678.
18. A. Y. Ledneva, S. B. Artemkina, D. A. Piryazev and V. E. Fedorov, *J. Struct. Chem.*, 2015, **56**, 1021–1023.
19. C. L. Raston and A. H. White, *Aust. J. Chem.*, 1979, **32**, 507–512.
20. A. Y. Ledneva, S. B. Artemkina, P. A. Stabnikov, L. V. Yanshole and V. E. Fedorov, *J. Struct. Chem.*, 2017, **58**, 758–762.
21. D. H. Johnston, C. King, A. Seitz and M. Sethi, *IUCrData*, 2021, **6**, 210778.
22. S. Evans, A. Hamnett, A. F. Orchard and D. R. Lloyd, *Faraday Discuss. Chem. Soc.*, 1972, **54**, 227–250.
23. S. J. Smith, C. M. Whaley, T. B. Rauchfuss and S. R. Wilson, *Inorg. Chem.*, 2006, **45**, 679–687.
24. S. Salamone, C. Colin, I. Grillier-Vuissoz, S. Kuntz, S. Mazerbourg, S. Flament, H. Martin, L. Richert, Y. Chapleur and M. Boisbrun, *Eur. J. Med. Chem.*, 2012, **51**, 206–215.
25. M. Sawa and H. Harada, *Curr. Med. Chem.*, 2006, **13**, 25–37.
26. M. M. Singh, *Med. Res. Rev.*, 2001, **21**, 302–347.
27. Y. Yamamoto and K. Itonaga, *Org. Lett.*, 2009, **11**, 717–720.
28. S. Madabhushi, R. Jillella, K. R. Godala, K. K. R. Mallu, C. R. Beeram and N. Chinthala, *Tetrahedron Lett.*, 2012, **53**, 5275–5279.
29. Y. Ishino, M. Miura, N. Hayakawa, T. Miyata, Y. Kaneko and T. Miyata, *Synth. Commun.*, 2001, **31**, 439–448.

